Journal of Alloys and Compounds 480 (2009) 938–941

Contents lists available at ScienceDirect

Journal of Alloys and Compounds

journal homepage: www.elsevier.com/locate/jallcom

Crystallization behaviors of TiO_2 films derived from thermal oxidation of evaporated and sputtered titanium films

Yuanyuan Zhang, Xiangyang Ma, Peiliang Chen, Deren Yang*

State Key Laboratory of Silicon Materials, Department of Materials Science and Engineering, Zhejiang University, Hangzhou 310027, China

ARTICLE INFO

Article history:
Received 20 October 2008
Received in revised form 17 February 2009
Accepted 21 February 2009
Available online 5 March 2009

Keywords:
Thin films
Crystal structure and symmetry
Thermal analysis

ABSTRACT

TiO_2 films were formed by thermal oxidation of electron-beam-evaporated and magnetron-sputtered titanium (Ti) films. It was found that the TiO_2 films formed by thermal oxidation of evaporated Ti films at 450 °C were of rutile phase, while those derived from thermal oxidation of sputtered Ti films at 450–600 °C kept to be of anatase phase. Such different crystallization behaviors of TiO_2 films seem to be due to the difference between the microstructures of evaporated and sputtered Ti films. Furthermore, the mechanism underlying the different crystallization behaviors of TiO_2 films has been tentatively explored.

1. Introduction

TiO_2 films have been widely applied in catalysis, solar cells, optical and electronic devices because of their desirable optical and electronic properties [1–4]. Generally, TiO_2 exhibits three crystal structures, i.e. anatase, brookite and rutile. The former two structures are thermodynamically unstable, while the latter one is stable [5–7]. A variety of routes such as sol–gel process, sputtering, electron beam evaporation, chemical vapor deposition (CVD) and thermal oxidation have already been used to prepare TiO_2 films [8–14]. Among them, thermal oxidation is relatively simple to prepare TiO_2 films. The crystallization behaviors of TiO_2 films formed by thermal oxidation of Ti films have been investigated previously. Hass et al. found that rutile TiO_2 films were formed at 400–450 °C by thermal oxidation of the Ti films deposited by fast evaporation under high vacuum, while anatase TiO_2 films were formed by thermal oxidation of the Ti films deposited by slow evaporation under poor vacuum [14]. Other research groups reported that rutile TiO_2 films were formed by thermal oxidation of sputtered Ti films at 500–550 °C [15–19]. However, the mechanism for the crystallization behaviors of TiO_2 films derived from thermal oxidation of evaporated and sputtered Ti films has not been addressed in the above-mentioned investigations.

In this work, we have studied the crystallization behaviors of TiO_2 films formed by thermal oxidation of evaporated and sputtered Ti films. It was found that TiO_2 films formed by thermal oxidation of evaporated Ti films at 450 °C were of rutile phase, while those derived from thermal oxidation of sputtered Ti films at 450–600 °C kept to be of anatase phase. The possible origin of this phenomenon has been tentatively explored.

2. Experimental

Ti films were prepared by electron beam evaporation and direct current (DC) magnetron sputtering, respectively, on ⟨1 0 0⟩ oriented p-type polished silicon substrates. Prior to being loaded into the chamber, the silicon substrates were cleaned by the standard RCA method [20]. For the evaporation of Ti films, the chamber was evacuated to 5×10^{-3} Pa and the electron beam was accelerated by a voltage of 8 kV. ~150-nm thick Ti films were evaporated on the non-heated substrates at a rate of 0.2 nm/s. For the sputtering of Ti films, the chamber was firstly evacuated to 5×10^{-3} Pa and then charged with argon gas at a flux of 30 sccm to reach a controlled working pressure of ~0.8 Pa. ~100-nm thick Ti films were sputtered on the non-heated substrates at a rate of 0.15 nm/s using a 99.9% pure titanium target. Subsequently, the deposited Ti films were oxidized at 400–600 °C for 5 h under oxygen ambient to form TiO_2 films.

The crystal structures of Ti films and TiO_2 films were analyzed by a D/max-rA, Rigaku X-ray diffractometer (XRD) using a Cu Kα radiation. The morphologies of Ti films and TiO_2 films were analyzed by a JEM-2010 transmission electron microscope (TEM) and a SIRION-100 field emission scanning electron microscope (FESEM). Regarding the preparation of specimens for the TEM observation, the silicon substrates were firstly grinded to be ~40 μm. Subsequently, an ion beam thinner was used to drill a hole initiating from the silicon substrates. The TEM observation was performed on the areas around the hole.

3. Results and discussion

Fig. 1(a) shows the XRD patterns of the films obtained by thermal oxidation of evaporated and sputtered Ti films at 500 °C for 5 h. All of the peaks in the XRD patterns 1 and 2 can be respectively indexed into anatase and rutile TiO_2 phases, indicating that the evaporated

* Corresponding author. Tel.: +86 571 87951667; fax: +86 571 87952322.
E-mail addresses: mxyoung@zju.edu.cn (X. Ma), mseyang@zju.edu.cn (D. Yang).

0925-8388/$ – see front matter.
doi:10.1016/j.jallcom.2009.02.100

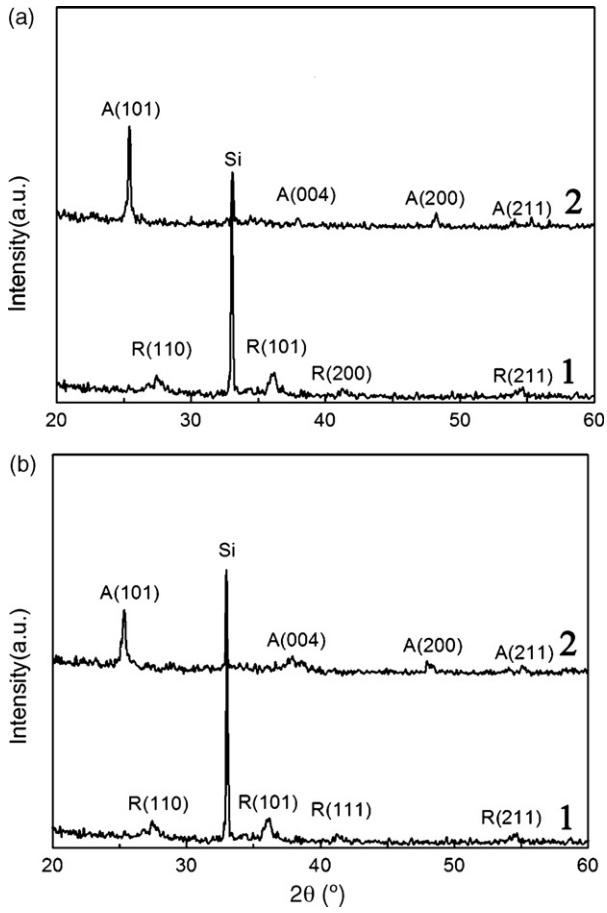

Fig. 1. XRD patterns of the TiO_2 films formed by thermal oxidation of (a) as-deposited Ti films and (b) Ti films pre-annealed at 500 °C for 2 h under a vacuum of 5×10^{-3} Pa. Thermal oxidation was performed under oxygen ambient at 500 °C for 5 h. 1 and 2 denote evaporated and sputtered Ti films, respectively. A and R denote anatase and rutile, respectively.

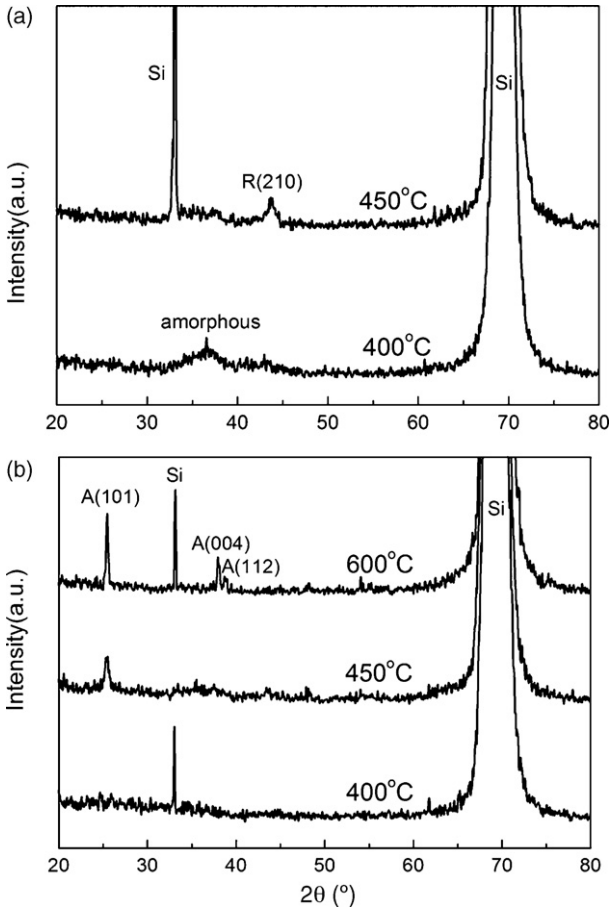

Fig. 2. XRD patterns of the TiO_2 films formed by thermal oxidation of (a) evaporated Ti films and (b) sputtered Ti films at different temperatures. A and R denote anatase and rutile, respectively.

and sputtered Ti films were substantially transformed into TiO_2 films by thermal oxidation. It can be seen from Fig. 1(a) that the rutile and anatase TiO_2 films were formed by thermal oxidation of evaporated and sputtered Ti films, respectively.

Generally, there are stresses between the deposited Ti films and the substrates. In order to clarify the effects of stresses on the crystallization behaviors of TiO_2 films formed by thermal oxidation of Ti films, the evaporated and sputtered Ti films were firstly annealed at 500 °C for 2 h under a vacuum of 5×10^{-3} Pa and then cooled slowly in order to relax the stresses. Subsequently, such pre-annealed Ti films were further oxidized at 500 °C for 5 h under oxygen ambient. The XRD patterns for the resulting films are shown in Fig. 1(b). The comparison between Fig. 1(a) and (b) indicates that the pre-annealing of Ti films under the vacuum has no effect on the crystallization behaviors of TiO_2 films. Accordingly, it is reasonably believed that the stresses between the deposited Ti films and the substrates do not substantially affect the crystallization behaviors of TiO_2 films.

Fig. 2 shows the XRD patterns of the films derived from thermal oxidation of evaporated and sputtered Ti films at 400–600 °C for 5 h. It can be seen that: (1) thermal oxidation of evaporated and sputtered Ti films at 400 °C just led to amorphous TiO_2 films; (2) the rutile TiO_2 films could be formed by thermal oxidation of evaporated films at 450 °C; and (3) thermal oxidation of sputtered Ti films at 450–600 °C resulted in the anatase TiO_2 films.

Thus far, it has been experimentally found that the rutile TiO_2 films can be formed by thermal oxidation of evaporated Ti films even at a low temperature of 450 °C, while the TiO_2 films derived from thermal oxidation of sputtered Ti films at 450–600 °C kept to be of anatase phase. Moreover, the stresses between the Ti films and substrates have been proved not to affect the crystallization behavior of TiO_2 films. Then, what factors leading to the difference between the crystallization behaviors of TiO_2 films derived from thermal oxidation of evaporated and sputtered Ti films, as reported herein, need to be further explored. In the following, based on the investigation of the microstructures of evaporated and sputtered Ti films and TiO_2 films, we have tentatively explained the crystallization behaviors of TiO_2 films.

Fig. 3(a) and (b) show the TEM images of evaporated and sputtered Ti films. Fig. 3(a) shows that within the evaporated Ti film quite a few Ti crystallites sized in 8–10 nm aggregate into "clusters", which are separated. On the other hand, as shown in Fig. 3(b), within the sputtered Ti film nearly all Ti crystallites sized in 4–5 nm amalgamate. The insets of Fig. 3(a) and (b) show the selective area electron diffraction (SAED) images taken on the evaporated and sputtered Ti films, respectively. Both SAED patterns can be indexed into hexagonal phase. Note that the brightest rings in the SAED patterns for the evaporated and sputtered Ti films correspond to (0 0 2) and (1 0 0) planes, respectively. Fig. 3(c) shows the XRD patterns of evaporated and sputtered Ti films. It can be seen that the most significant peaks in the XRD patterns of evaporated and sputtered Ti films correspond to (0 0 2) and (1 0 0) planes, respectively, which are manifested by the brightest rings in the corresponding SAED patterns, as mentioned above. It should be pointed out that other indexed planes in the SAED patterns shown in Fig. 3(a) and (b) are not revealed in the XRD patterns, which is most likely due to the

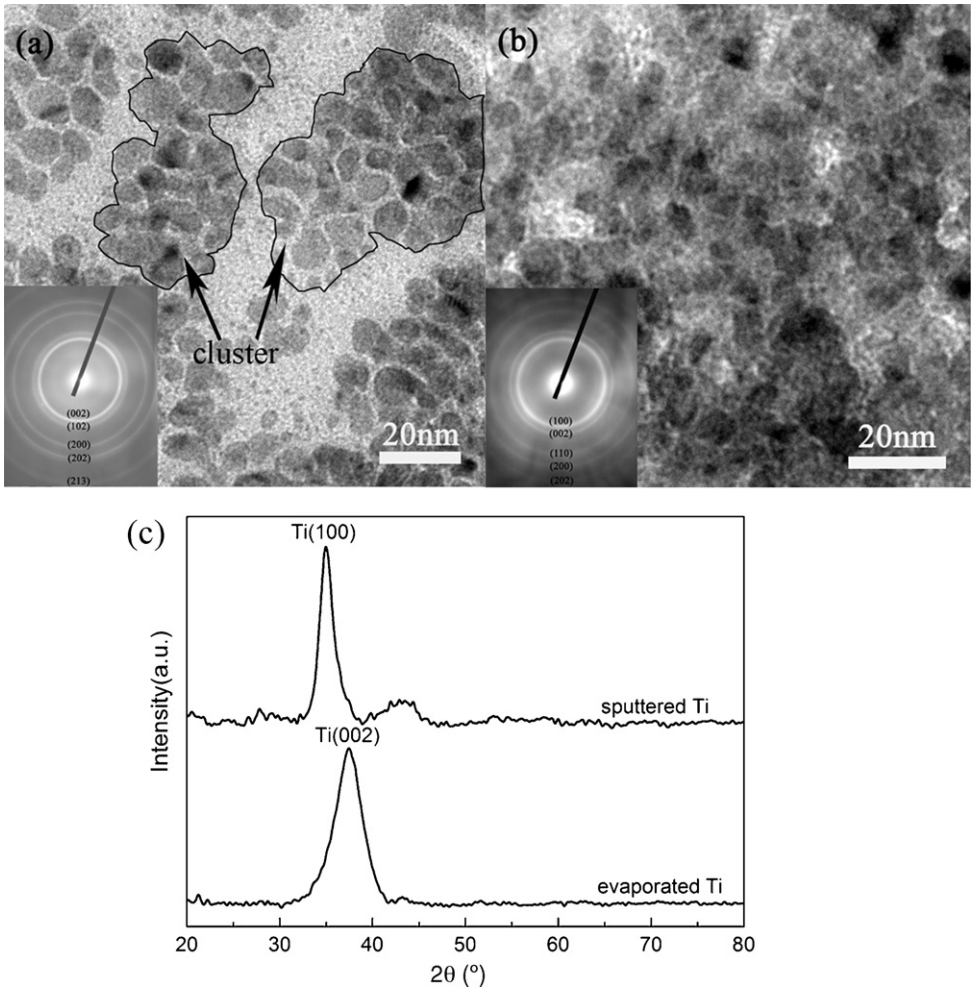

Fig. 3. TEM images of (a) evaporated and (b) sputtered Ti films, the insets show the selective area electron diffraction (SAED) images of evaporated and sputtered Ti films, respectively. (c) XRD patterns of evaporated and sputtered Ti films.

fact that the evaporated and sputtered Ti films were too thin. Moreover, the diffraction peaks in the XRD pattern for the evaporated Ti film are broader than those for the sputtered Ti film, as shown in Fig. 3(c). This indicates that the sputtered Ti films were crystallized better than the evaporated ones.

Fig. 4(a) and (b) show the SEM images of the evaporated and sputtered Ti films, respectively. The comparison between Fig. 4(a) and (b) reveals that the sputtered Ti film is denser than the evaporated one. Moreover, the Ti particles sized in ~5 nm within the sputtered film are smaller than those sized in ~10 nm within the evaporated one. Fig. 4(c) and (d) show the SEM images of the TiO_2 films formed by thermal oxidation of evaporated and sputtered Ti films at 500 °C for 5 h, respectively. It can be seen that the TiO_2 film derived from sputtered Ti film is much denser and possesses much smaller grains with respect to that derived from evaporated Ti film. The difference between the microstructures of TiO_2 films, as mentioned above, is most likely due to the different microstructures of the evaporated and sputtered Ti films. Although the different crystallization behaviors of TiO_2 films, as mentioned above, have not been essentially understood, we will tentatively give a phenomenological explanation as below.

Regarding the oxidation of Ti films, on a microscopic scale, it firstly occurs on the surface and boundary of each Ti grain [21,22]. After sufficient oxidation, each Ti grain is transformed into a TiO_2 crystallite. Therefore, in a way, the Ti grains can be regarded as the nuclei for TiO_2 crystallites. It should be noted that the molar volume of TiO_2 is larger than that of Ti. Consequently, the stresses will generate during the oxidation of Ti. On the other hand, for TiO_2, rutile is thermodynamically stable relative to anatase by $\Delta G_{bulk} \approx 67$ kJ/mol [23]. However, the resulting phase of TiO_2 depends on the temperature and even the grain/particle size [6,23]. Overall, at temperatures lower than 600 °C, anatase TiO_2 readily forms; while, rutile TiO_2 forms at higher temperatures. Zhang et al. have investigated the phase transformation for TiO_2 nanoparticles. Their thermodynamic analyses and experimental investigations have proved that at appropriate temperatures the crossover in phase stability occurs around a critical particle size ($D_c \approx 10$–15 nm) [23–25], that is, rutile forms above D_c while anatase is stable below D_c due to the surface contribution. Based on their results, we can preliminarily understand the crystallization behaviors of TiO_2 films derived from oxidation of Ti films, as reported herein. As for the evaporated Ti films, the grains are relatively large (~10 nm, see Figs. 3(a) and 4(a)). Therefore, the resulting TiO_2 grains are relatively large (~50 nm, see Fig. 4(c)). Moreover, the grains within the evaporated Ti film are not adjoined each other (see Fig. 3(a)), which facilitates the relief of stresses arising from the oxidation of Ti grains and therefore the growth of TiO_2 grains. Therefore, according to the thermodynamic analysis performed by Zhang et al. [6,21–24], rutile TiO_2 can form. Regarding the sputtered Ti films, the grains are much smaller (~5 nm, see Figs. 3(b) and 4(b)) and most of them join each other. Therefore, the resulting TiO_2 grains are small. Moreover, there are no substantial spaces for the TiO_2 grains to coarsen. In this case, the surface energies of TiO_2 grains increase significantly to be favorable for the formation of

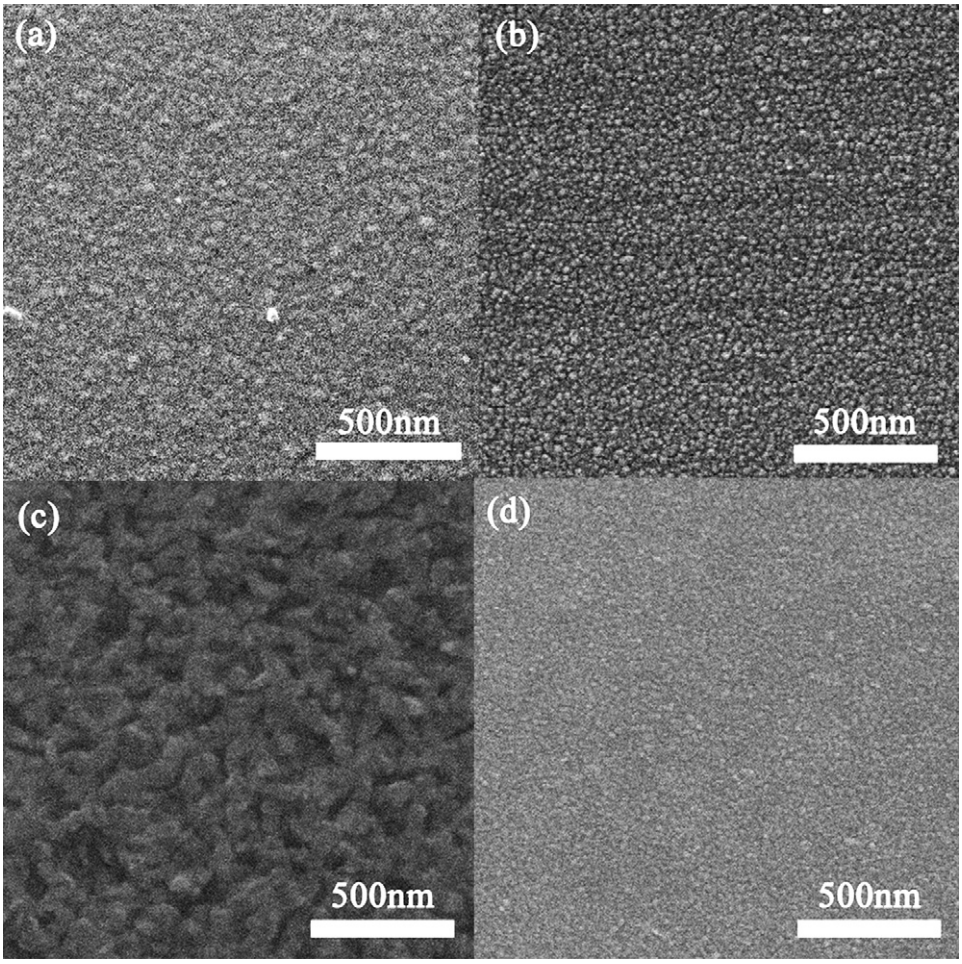

Fig. 4. SEM images of (a) evaporated Ti film, and (b) sputtered Ti film, (c) and (d) TiO_2 films respectively derived from thermal oxidation of evaporated and sputtered Ti films.

anatase [26]. It should be stated that in-depth understanding of the crystallization behaviors of TiO_2 films prepared by oxidation of sputtered and evaporated Ti films needs more elaborate investigations.

4. Conclusions

The crystallization behaviors of TiO_2 films formed by thermal oxidation of evaporated and sputtered Ti films have been investigated. It was found that the TiO_2 films resulting from thermal oxidation of evaporated Ti films at 450 °C were of rutile phase, while those generated by thermal oxidation of sputtered Ti films at 450–600 °C kept to be of anatase phase. Such different crystallization behaviors of TiO_2 films are most likely due to the different microstructures of evaporated and sputtered Ti films. According to the basic idea of previously reported thermodynamic analysis on the phase transformation of TiO_2 nanoparticles, we have tentatively explored the underlying mechanism for the different crystallization behaviors of TiO_2 films.

Acknowledgements

The authors would like to thank the financial supports from the Research Fund for Doctoral Program of Higher Education of China (No. 007033501), "973 project" (No. 2007CB613403) and programs for New Century Excellent Talents in Universities and Changjiang Scholar and Innovative Team.

References

[1] T. Thompson, J.T. Yates Jr., Chem. Rev. 106 (2006) 4428.
[2] M. Pal, J.G. Serrano, P. Santiago, U. Pal, J. Phys. Chem. C 111 (2007) 96.
[3] S. Ito, T.N. Murakami, P. Comte, P. Liska, C. Grätzel, M.K. Nazeeruddin, M. Grätzel, Thin Solid Films 516 (2008) 4613.
[4] B.R. Weinberger, R.B. Garber, Appl. Phys. Lett. 66 (1995) 2409.
[5] J. Zhang, M.J. Li, Z.C. Feng, J. Chen, C. Li, J. Phys. Chem. B 110 (2006) 927.
[6] H.Z. Zhang, J.F. Banfield, J. Mater. Res. 15 (2000) 437.
[7] D.J. Reidy, J.D. Holmes, M.A. Morris, Ceram. Int. 32 (2006) 235.
[8] N. Wethakun, S. Phanichphant, Curr. Appl. Phys. 8 (2008) 343.
[9] H. Ogawa, T. Higuchi, A. Nakamura, S. Tokita, D. Miyazaki, T. Hattori, T. Tsukamoto, J. Alloys Compd. 449 (2008) 375.
[10] Q. Li, J.K. Shang, J. Am. Ceram. Soc. 9 (2008) 3167.
[11] E.M. Assim, J. Alloys Compd. 463 (2008) 55.
[12] M.G. Rocha, A.C. Gallardo, I.H. Calderon, Mod. Phys. Lett. B 15 (2001) 769.
[13] G. Ji, Z. Zhang, Y. Liu, X.D. Ding, J. Sun, X.B. Ren, J. Alloys Compd. 448 (2008) 171.
[14] G. Hass, Vacuum 11 (1952) 331.
[15] C.C. Ting, S.Y. Chen, D.M. Liu, J. Appl. Phys. 88 (2000) 4628.
[16] Y. Sun, Appl. Surf. Sci. 233 (2004) 328.
[17] D.S.R. Krishna, Y. Sun, Surf. Coat. Technol. 198 (2005) 447.
[18] C.C. Ting, S.Y. Chen, D.M. Liu, Thin Solid Films 402 (2002) 290.
[19] D.S.R. Krishna, Y. Sun, Appl. Surf. Sci. 252 (2005) 1107.
[20] W. Kern, Handbook of Semiconductor Wafer Cleaning Technology: Science, Technology, and Applications, Noyes, Park Ridge, NJ, 1993.
[21] B. Gilbert, H.Z. Zhang, F. Huang, M.P. Finnegan, G.A. Waychunas, J.F. Banfield, Geochem. Trans. 4 (2003) 20.
[22] H. Zhang, J.F. Banfield, Am. Miner. 84 (1999) 528.
[23] H. Zhang, J.F. Banfield, J. Phys. Chem. B 104 (2000) 3481.
[24] H. Zhang, J.F. Banfield, J. Mater. Chem. 8 (1998) 2073.
[25] A.A. Gribb, J.F. Banfield, Am. Miner. 82 (1997) 717.
[26] P. Nair, F. Mizukami, T. Okubo, J. Nair, K. Keizer, A.J. Burggraaf, Ceram. Process. 43 (1997) 2710.